Open access • Proceedings Article • DOI:10.23919/ECC.2009.7075065

Multi-sensor longitudinal control with fault tolerant guarantees — Source link

John J. Martinez, Maria M. Seron, José A. De Doná

Institutions: Grenoble Institute of Technology, University of Newcastle

Published on: 23 Aug 2009 - European Control Conference

Multi-Sensor Longitudinal Control with Fault Tolerant Guarantees

John J. Martínez, María M. Seron and José A. De Doná

Abstract— **This paper deals with the problem of obtaining fault-tolerant guarantees of a multi-sensor switching strategy for longitudinal control. The strategy selects, at each instant of time, the sensor (belonging to a collection of sensors) that provides the best closed loop performance, as measured by a control-performance criterion. It is assumed that each sensor has an associated feedback controller that has been designed such that the sensor-controller pair stabilises the closed loop system under normal operation conditions. Recent refinements for constructing ultimate-bound invariant sets allow obtaining less conservative fault-tolerant guarantees. Stability of the switching system under fault-free operation conditions and under presence of sensor failures are established in the main results of this paper.**

I. INTRODUCTION

The problem of longitudinal control in automotive applications has attracted considerable recent attention from the control research community [4]. The problem consists in automatically keeping, within certain safe range, the distance of a *follower* car with respect to a *leader* car.[1] This distance must be kept despite the possible driving maneuvers of the leader car while, at the same time, maintaining the level of comfort of the passengers of the follower vehicle [5].

A longitudinal controller is generally composed by two loops: an inner control loop which compensates the nonlinear vehicle dynamics (throttle and brake), and an outer control loop which ensures good tracking of the desired inter-distance reference. Here we are only interested in the outer inter-distance control loop.

In general, the vehicle inter-distance is measured using sensors of different nature, bandwidth, accuracy and noise levels. Examples of sensors are automotive lasers, radars and stereo-vision (see Figure 1). Each of these types of sensors has a good performance in specific operating or environmental conditions. However, during certain periods of time one sensor could fail or operate outside its specified operating conditions. Vision systems, in particular, are not reliable for inter-distance detection in bad weather conditions because of misinterpretation problems and operation faults. For instance, stereo-vision fails when the car is travelling inside a tunnel. On the other hand, radar systems offer relatively accurate inter-distance information and robustness in bad weather, but their performance in terms of spatial resolution is poor. Thus, a single sensor is not adequate to provide reliable information for autonomous driving guidance in real time due to changing weather, ambient lighting, and other limitations.

The problem is then how to negotiate these difficulties in order to guarantee that the complete system is still stable and the performance is still maintained within acceptable values. A sensible approach is to use multiple sensors with different characteristics so as to improve the performance of individual sensors and obtain a better estimation of the plant states. A classical way of combining multiple sensors has been the fusion of sensors in a unique overall state estimator [6]–[8]. However, in automotive control, the operation conditions or the environment constraints could change frequently and it is very difficult to predict how the sensors will work at each instant of time. For example, a particular sensor could fail and, if the sensor fusion scheme does not recognize this situation, the results could be potentially disastrous.

Another possible approach that could solve some of the difficulties associated with using multiple sensors is to use models of healthy plant-sensor in order to identify when a sensor fails and commute to another one, preserving the operability of the system. This approach is extensively cited in the fault-tolerant control literature (a survey is given in [10], and an example is given in [9]). However, the main drawback of this method is related to the necessity to calculate all possible controllers for all possible operation failures, see for example [11].

This paper deals with the problem of obtaining fault-tolerant guarantees of a multi-sensor switching strategy for longitudinal control. The strategy selects, at each instant of time, the sensor (belonging to a collection of sensors) that provides the best closed loop performance, as measured by a control-performance criterion. It is assumed that each sensor has an associated feedback controller that has been designed such that the sensor-controller pair stabilises the closed loop system under normal operation conditions. Stability of the switching system under normal (fault-free) operation and in the presence of sensor failures is established in this paper.

This paper follows similar lines as the scheme already presented by the authors in [1], [2] and [14]. The main differences are as follows:

(i) The control design proposed here is based on Lyapunov techniques (see (16)–(17)), instead of requiring to solve a Riccati equation. This shows the generality of the scheme, afforded by the use of invariant sets for the determination of fault tolerance guarantees, which are expressed in terms of a separation condition on these sets.

(ii) The design of the estimators is simplified, since here we utilise standard estimators in predictor form, instead of

J.J. Martínez is with Département Automatique, GIPSA-lab UMR 5216, Grenoble-INP, France. jairo.martinez@grenoble-inp.fr

M.M. Seron and J.A. De Doná are with the Centre for Complex Dynamic Systems and Control, School of EE&CS, The University of Newcastle, Australia. J.A. De Doná is currently on study leave with a visiting position at CAS, Mathématiques et Systèmes, Mines-ParisTech, France.

[1] The problem could also comprise more than two cars, however this paper concentrates on the two-vehicle problem.

ISBN 978-963-311-369-1

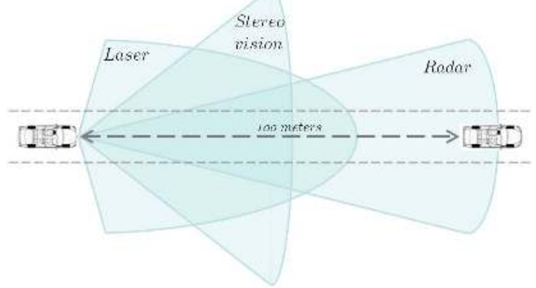

Fig. 1. Multi-sensor regions for automotive longitudinal control.

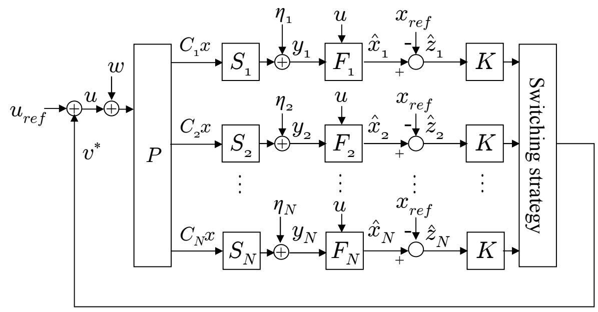

Fig. 2. Multisensor switching scheme with plant P, sensors $S_1, \ldots S_N$, estimators $F_1, \ldots, F_N$ and feedback gain K.

requiring prediction-correction schemes. This allows to simplify the stability and fault tolerance analyses and, moreover, to obtain less conservative set separation conditions.

(iii) We make use, in the simulation example, of techniques recently developed by the authors in [13] to refine the construction of the invariant sets.

As a consequence of the ensuing reduction of conservatism, we are in this work able to tackle more demanding operation conditions in the vehicle longitudinal control example studied. In effect, in this paper we present fault tolerant guarantees for a *stop-and-go* driving scenario. Such driving situations, in the presence of sensor faults, had not been analysed theoretically in [1] and, in that sense, this paper completes that work. On the other hand, the theoretical analysis done in [2] and [14] only covered the *car-following* scenario for longitudinal control, hence that work is completed by the present paper as well.

II. Switching control scheme

In this section we describe the proposed switching control scheme, depicted in Figure 2.

A. The inter-distance dynamics - The plant

The inter-distance dynamics can be represented as a double integrator driven by the difference between the leader vehicle acceleration a_l and the follower vehicle acceleration a_f, i.e.,

$$\ddot{d} = a_l - a_f, \tag{1}$$

where d is the distance between the two vehicles.

Defining the control input $u \triangleq \hat{a}_l - a_f$, where $\hat{a}_l$ stands for an estimation of the leader vehicle acceleration, (1) can be expressed as

$$\ddot{d} = u + \tilde{a}_l, \tag{2}$$

where $\tilde{a}_l \triangleq a_l - \hat{a}_l$ is seen as a perturbation signal.

Finally, defining $x \triangleq [d\ \dot{d}]'$ and $w \triangleq \tilde{a}_l$, and discretising the system, the inter-distance dynamics can be described by the following linear discrete-time model:

$$x^+ = Ax + Bu + Ew, \tag{3}$$

where $x \in \mathbb{R}^2$ and $x^+ \in \mathbb{R}^2$ are, respectively, the current and successor system states, $u \in \mathbb{R}^1$ is the input, and $w \in \mathbb{R}^1$ is a bounded process disturbance.

Remark 2.1: The pair (A, B) is stabilisable. ◦

B. The reference model

The inter-distance reference model is taken as an exosystem describing a *virtual* vehicle dynamics which is positioned at a distance d^r (the reference distance) from the leader vehicle. The reference model dynamics are given by

$$\ddot{d}^r = \hat{a}_l - a_f^r(d^r, \dot{d}^r), \tag{4}$$

where $a_f^r(d^r, \dot{d}^r)$ is a nonlinear function of the inter-distance reference d^r and its time-derivative $\dot{d}^r$. This function can be designed to meet safety and comfort requirements, as is proposed in [5]. Here we will assume that the function $a_f^r(.)$ is given. Taking $u_{ref} \triangleq \hat{a}_l - a_f^r(d^r, \dot{d}^r)$, we have

$$\ddot{d}^r = u_{ref}. \tag{5}$$

Thus, defining $x_{ref} \triangleq [d^r\ \dot{d}^r]'$, and analogously to the step from (2) to (3) above, the reference system will be described by the following linear discrete-time model:

$$x_{ref}^+ = Ax_{ref} + Bu_{ref}. \tag{6}$$

Notice that we have conserved the same structure for both the inter-distance dynamics and the inter-distance reference model, with same matrices A and B.

Assumption 2.2: (Reference bounds). The reference signals u_{ref} and x_{ref} in (6) are bounded. In particular, constant vectors $x_{ref}^0 \in \mathbb{R}^2$ and $\bar{x}_{ref} \in \mathbb{R}^2$ are known such that $x_{ref}(k) \in X_{ref} \triangleq \{x_{ref} \in \mathbb{R}^2 : |x_{ref} - x_{ref}^0| \leq \bar{x}_{ref}\}$. ◦

Note that, since matrix A has eigenvalues on the unit circle, u_{ref} must be obtained from a stabilising feedback controller for system (6).

C. Inter-distance control objective

The control objective is for the state of the plant (3) to track an inter-distance reference signal x_{ref} that satisfies (6). We will study the plant tracking error defined as

$$z \triangleq x - x_{ref}. \tag{7}$$

In addition, we define the tracking error for the input as

$$v \triangleq u - u_{ref}. \tag{8}$$

Then, from (3), (6), (7) and (8), the plant tracking error dynamics is described by

$$z^+ = Az + Bv + Ew. \tag{9}$$

The control objective could be then re-interpreted as follows: Find at each time instant an appropriate control input v such that the tracking error z is bounded in the presence of bounded disturbances w. From a practical point of view, the full state is not always available. Then, we will analyse the control of the system (9) by means of sensors and estimators. In the following section, we propose a multi-sensor switching control scheme to achieve this objective.

D. Multi-sensors and Multi-estimators

We assume that the output of system (3) is measured via a family of N sensors

$$y_i = C_i x + \eta_i, \qquad i = 1, \cdots, N, \tag{10}$$

where, $y_i \in \mathbb{R}^{p_i}$ is the measured output and $\eta_i \in \mathbb{R}^{p_i}$ is a bounded measurement disturbance.

Assumption 2.3: The pairs (A, C_i) are detectable for $i = 1, \ldots, N$. ◦

We consider N state estimators, each of which estimates the states of the plant. The estimators are described by the following equations, for $i = 1, \cdots, N$:

$$\hat{x}_i^+ = A\hat{x}_i + Bu + L_i(y_i - C_i\hat{x}_i), \tag{11}$$

Assumption 2.4: The gains L_i are such that

$$A_{L_i} \triangleq A - L_i C_i \tag{12}$$

for $i = 1, \cdots, N$, have their eigenvalues strictly inside the unit circle [this is always possible by Assumption 2.3][2]. ◦

Remark 2.5: The estimation errors, defined as

$$\tilde{x}_i \triangleq x - \hat{x}_i, \quad i = 1, \cdots, N, \tag{13}$$

satisfy, using (3), (10), (11), and (12),

$$\tilde{x}_i^+ = A_{L_i}\tilde{x}_i + Ew - L_i\eta_i \tag{14}$$

Hence, it follows from Assumption 2.4 that $\tilde{x}_i$ are bounded whenever w and η_i are bounded. ◦

E. Multi-controllers

We define the tracking error for the state estimates as:

$$\hat{z}_i \triangleq \hat{x}_i - x_{ref}, \quad i = 1, \cdots, N. \tag{15}$$

Then, to each sensor-estimator pair we associate a feedback controller of the form:

$$v_i = -K\hat{z}_i, \quad i = 1, \cdots, N. \tag{16}$$

Assumption 2.6: The gain K is stabilising, that is, the matrix $(A-BK)$ has all its eigenvalues inside the unit circle, and the pair (K, P) satisfies the Lyapunov equation

$$(A - BK)'P(A - BK) - P = -Q \tag{17}$$

for a given positive definite matrix Q. ◦

[2]If the estimators are steady-state Kalman filters then L_i is obtained via an algebraic Riccati equation. More generally, L_i can be computed by placement of the poles of A_{L_i} in some desired location.

F. Switching strategy

We propose a switching strategy that at each time instant selects a suitable feedback control as follows:

$$v = -K\hat{z}_l, \tag{18}$$

for l defined as

$$l \triangleq \arg \min_{i=1,\cdots,N.} \{\hat{z}_i' P \hat{z}_i\}, \tag{19}$$

where P satisfies Assumption 2.6. In the sequel we refer to the index l as the switching signal.

Thus, at each time instant, the switching strategy selects the feedback control (18) that achieves the smallest value $\hat{z}_l' P \hat{z}_l$ of the "switching performance criterion" in (19).

III. Stability in presence of bounded disturbances

In this section we prove closed-loop stability of the switching scheme described in Section II. From (7), (13) and (15), the estimation tracking error can be expressed as

$$\hat{z}_i = z - \tilde{x}_i, \quad i = 1, \cdots, N. \tag{20}$$

Then, system (9) in feedback with (18) can be written as

$$z^+ = (A - BK)z + BK\tilde{x}_l + Ew. \tag{21}$$

Hence, it follows from Assumption 2.6 that z is bounded whenever $\tilde{x}_l$ and w are bounded.

On the other hand, from definition (15), and using (6), (8), (10), (11), (12), (13), (18) and (20) we have:

$$\hat{z}_i^+ = A_{L_i}\hat{z}_i + (L_iC_i - BK)z + BK\tilde{x}_l + L_i\eta_i, \tag{22}$$

for $i = 1, \cdots, N$. Hence, it follows from Assumption 2.4 that $\hat{z}_i$ are bounded whenever z, $\tilde{x}_l$ and η_i are bounded.

A. Ultimate bounds

We present below a theorem (see [12], [14]) that will allow us to compute ultimate bounds for the closed-loop system's states. In the sequel, $|\,M\,|$ denotes the elementwise magnitude of a (possibly complex) matrix M; $x \leq y$ ($x < y$) denotes the set of elementwise (strict) inequalities between the components of the real vectors x and y; if $W_l = \left[w_l^1 \; \ldots \; w_l^n\right]'$, $l \in \{1, \ldots, N\}$, are vectors in $\mathbb{R}^n$ then $\max_{l\in\{1,\ldots,N\}} W_l$ denotes the elementwise maximum, whose ith element, $i = 1, \ldots, n$, is defined as

$$\left(\max_{l\in\{1,\ldots,N\}} W_l\right)_i \triangleq \max\{w_1^i, \ldots w_N^i\}. \tag{23}$$

Theorem 3.1: Consider the system $x(k + 1) = Ax(k) + B_l\nu_l(k)$, where $A \in \mathbb{R}^{n\times n}$, $B_l \in \mathbb{R}^{n\times m}$, $l \in \{1, \ldots, N\}$, and A has eigenvalues strictly inside the unit circle. Let $V\Lambda V^{-1}$ be the Jordan matrix decomposition of A. Assume that, for all $l \in \{1, \ldots, N\}$, $|\,\nu_l(k)\,| \leq \bar{\nu}_l$ for all $k \geq 0$, where $\bar{\nu}_l \in \mathbb{R}^m$, $\bar{\nu}_l > 0$, and let $\bar{\nu} \triangleq \max_{l\in\{1,\ldots,N\}} |\,V^{-1}B_l\,|\bar{\nu}_l$. For $\epsilon \in \mathbb{R}^n$, $\epsilon \geq 0$, define

$$S_\epsilon \triangleq \left\{x \in \mathbb{R}^n : \left|\,V^{-1}x\,\right| \leq (I - |\,\Lambda\,|)^{-1}\bar{\nu} + \epsilon\right\}. \tag{24}$$

Then:

1) For any $\epsilon \geq 0$, the set S_ϵ is (positively) invariant. That is, if $x(0) \in S_\epsilon$, then $x(k) \in S_\epsilon$ for all $k \geq 0$.
2) Given $\epsilon \in \mathbb{R}^n$, $\epsilon > 0$, there exists $k^* \geq 0$ such that $x(k) \in S_\epsilon$ for all $k \geq k^*$. ∘

Remark 3.2: Part 1 of Theorem 3.1 characterises invariant sets in the state space, the smallest being the set S_0 obtained by taking $\epsilon = 0$ in (24). Part 2 shows that the state trajectories asymptotically converge to the invariant set S_ϵ for $\epsilon \geq 0$ (in particular, S_0) from any initial condition. In addition, for $\epsilon > 0$, the state trajectories enter S_ϵ in finite time. Note that an elementwise ultimate bound on the state can be obtained from Theorem 3.1 using the fact that $|\, x(k) \,| \leq |\, V \,| \, \big|\, V^{-1}x(k) \,\big|$. ∘

Remark 3.3: If the eigenvalues of $A = V\Lambda V^{-1}$ are real, then the sets S_ϵ in (24) are polyhedral sets. ∘

Remark 3.4: Assume that bounds on the measurement disturbances $|\eta_i| \leq \bar{\eta}_i$, for $i = 1, \ldots, N$, and process disturbance $|w| \leq \bar{w}$ are problem data.[3] Applying Theorem 3.1 to the estimation error subsystems (14), we obtain the following invariant sets in which each subsystem's trajectories will remain if started inside or towards which the trajectories will asymptotically converge if started outside:

$$\tilde{S}_i \triangleq \Big\{ \tilde{x}_i \in \mathbb{R}^2 : \big|\, V_i^{-1} \tilde{x}_i \,\big| \leq (I - |\Lambda_i|)^{-1} \big| V_i^{-1} [E \quad -L_i] \big| \begin{bmatrix} \bar{w} \\ \bar{\eta}_i \end{bmatrix} \Big\}, \tag{25}$$

for $i = 1, \ldots, N$, where $A_{L_i} = V_i \Lambda_i V_i^{-1}$ is the Jordan decomposition of A_{L_i}. From (25), we can compute ultimate bounds on $\tilde{x}_i$, as suggested in Remark 3.2:

$$|\tilde{x}_i| \leq |V_i| (I - |\Lambda_i|)^{-1} \big| V_i^{-1} [E \quad -L_i] \big| \begin{bmatrix} \bar{w} \\ \bar{\eta}_i \end{bmatrix}. \tag{26}$$

Then, from (20)–(22) and the bounds (26), we can obtain ultimate bounds on z and $\hat{z}_i$, again using Theorem 3.1 and Remark 3.2,

$$\hat{S}_i \triangleq \big\{ \hat{z}_i \in \mathbb{R}^2 : \big|\, V_i^{-1} \hat{z}_i \,\big| \leq (I - |\Lambda_i|)^{-1} \big| V_i^{-1} [L_i C_i - BK \;\; BK \;\; L_i] \big| \, \bar{\nu}_{li} \big\}, \tag{27}$$

where $|\nu_{li}| \leq \bar{\nu}_{li}$ with $\nu_{li} \triangleq [z' \; \tilde{x}_l' \; \eta_i']'$. ∘

Remark 3.5: The ultimate-bound invariant sets of the form (25) and (27) are constructed using techniques developed in [12]. A refinement of those techniques was presented in [13], where a procedure was developed to obtain arbitrarily close approximations of the minimal robust positively invariant (mRPI) set for a stable system driven by bounded disturbances. ∘

IV. Closed-loop stability under sensor fault

A. Closed-loop dynamics during the fault

Our fault model is described in the following definition. We consider *abrupt* faults that lead to sensor *outage*.

[3]In the sequel, if $\nu(k) \in \mathbb{R}^m$ is a discrete-time signal and $\bar{\nu} \in \mathbb{R}^m$, $\bar{\nu} \geq 0$, then $|\nu| \leq \bar{\nu}$ denotes the elementwise bound $|\nu(k)| \leq \bar{\nu}$ for all times $k \geq k^*$, for some $k^* \geq 0$.

Definition 4.1: A sensor is *operational* (or "healthy") when its measured output is given by (10). When a jth sensor *fails* its measured output during the fault is given by

$$y_j = \eta_j^F, \tag{28}$$

where η_j^F is a bounded noise. ∘

In the following subsections we shall establish closed-loop stability under sensor fault by providing conditions that guarantee that the switching scheme never selects faulty sensors to implement the control law.

Assumption 4.2: (working hypothesis) The switching scheme (19) always selects only healthy sensors whose estimation errors satisfy (26). ∘

1) Healthy sensors: Provided only healthy sensors are selected by the switching controller, the closed-loop dynamics of the estimator tracking errors for each of the ith sensors that remain healthy continue to obey (22), that is, do not change in the event a jth sensor fails. Moreover, the bounds that define the sets $\hat{S}_i$, namely $|\nu_{li}| \leq \bar{\nu}_{li}$, remain valid while (26) holds for the selected sensor (see (27)). Thus, under Assumption 4.2, if the trajectories of healthy sensors (22) are evolving in the corresponding invariant set $\hat{S}_i$, then they remain in this set.

2) Faulty sensors: Assuming that the switching scheme only selects healthy sensors $l \in \{1, \cdots, N\}$, $l \neq j$, then using equations from Sections II and III together with (28), we have the following closed-loop estimator tracking error subsystems during the fault:

$$\hat{z}_j^+ = A_{L_j} \hat{z}_j + \gamma_{lj}^F, \quad j = 1, \ldots, N, \tag{29}$$

where $\gamma_{lj}^F \triangleq -BKz + BK\tilde{x}_l + L_j \eta_j^F - L_j C_j x_{ref}$ with l varying in $\{1, \ldots, N\}$, $l \neq j$.

Comparing (29) with (22), we observe that some of the inputs to the estimation tracking error subsystems have changed after the fault. However, under Assumption 4.2, the signals z, $\tilde{x}_l$, for all operational sensors $l \in \{1, \ldots, N\}$, $l \neq j$, satisfy the same bounds as before the fault. In addition, η_j^F, for $j = 1, \ldots, N$, and x_{ref} are bounded by assumption. Hence, as before, we can use these different bounds to obtain a bound $\bar{\nu}_{lj}^F$ such that $|\nu_{lj}^F| \leq \bar{\nu}_{lj}^F$. Using (24) (with $\epsilon = 0$) we can then compute the "under-fault" set

$$\hat{S}_j^F \triangleq \Big\{ \hat{z}_j \in \mathbb{R}^2 : \big| V_j^{-1} \hat{z}_j \big| \leq (I - |\Lambda_j|)^{-1} \max_{l \in \{1,\ldots,N\}} |V_j^{-1} B_j| \bar{\nu}_{lj}^F \Big\} \oplus \{\hat{z}_j^{F,0}\}, \tag{30}$$

where $\oplus$ denotes the Minkowski sum of sets, $B_j \triangleq [-BK \;\; BK \;\; L_j \;\; -L_j C_j]$, $\bar{\nu}_{lj}^F \triangleq [\bar{z}' \; \bar{\tilde{x}}_l' \; (\bar{\eta}_j^F)' \; \bar{x}_{ref}']'$, with $\bar{x}_{ref}$ as in Assumption 2.2, and where the offset $\hat{z}_j^{F,0}$, due to the offset x_{ref}^0 of x_{ref}, is computed as:

$$\hat{z}_j^{F,0} = -(I - A_{L_j})^{-1} L_j C_j x_{ref}^0. \tag{31}$$

Thus, it follows from Theorem 3.1 and the previous analysis that, under Assumption 4.2, the trajectories of (29) remain in $\hat{S}_j^F$ defined in (30) if started inside or will asymptotically converge towards $\hat{S}_j^F$ if started outside.

We are now ready to establish conditions to ensure that our working hypothesis (Assumption 4.2) is satisfied.

B. Conditions for closed-loop stability

The analysis of Section IV-A motivates us to impose the following assumption, which describes the less conservative fault scenario that allows us to obtain fault tolerance guarantees within the proposed framework.

Assumption 4.3 (Fault scenario):

1) At any time instant, at least one sensor is operational; in addition, all operational sensors have estimation errors inside the invariant sets $\tilde{S}_i$ (25) and estimation tracking errors inside the invariant sets $\hat{S}_i$ (27).
2) Any time a jth sensor fails, for any $j \in \{1, \ldots, N\}$, the states of the corresponding estimator tracking error subsystem (29), at the following sampling time, belong to the invariant set $\hat{S}_j^F$ (30). ○

We will now provide a way to verify Condition 2) of Assumption 4.3, using set definitions.

From (21) we can compute, using the techniques described in Section III, an invariant set, Z, such that $z \in Z$, whenever the chosen sensors are healthy. We can also construct bounding sets, N_j^F, for the bounded noises, such that $\eta_j^F \in N_j^F,\ j = 1, ..., N$. Then, assuming that the jth sensor has been healthy for sufficiently long time, so that $\hat{z}_j \in \hat{S}_j$, we can see from (29) that, the instant *after the occurrence of a fault*, the variable $\hat{z}_j$ will be in the following *after fault* transitional set:

$$\hat{S}_j^{H\to F} \triangleq A_{L_j}\hat{S}_j \oplus (-BK)Z \oplus BK \bigcup_{l=1}^{N} \tilde{S}_l \oplus L_j N_j^F \oplus (-L_jC_j)X_{ref}. \quad (32)$$

Finally, the following pre-checkable condition guarantees, in combination with Condition 1) of Assumption 4.3, that Condition 2) of Assumption 4.3 is satisfied.

Assumption 4.4: The sets (30) and (32) satisfy $\hat{S}_j^{H\to F} \subseteq \hat{S}_j^F$, for all $j = 1, ..., N$. ○

The following theorem provides conditions to guarantee closed-loop stability under sensor fault.

Theorem 4.5: Suppose that bounds on the sensor noises η_i, and on the "fault noises" η_i^F for $i = 1, \ldots, N$, are given in the form $\eta_i \in N_i$, and $\eta_i^F \in N_i^F$, respectively, where N_i and N_i^F are polyhedral sets. Suppose that Assumption 4.4 is satisfied and that the following conditions hold for all $j = 1, \ldots, N$:

$$\max_i \{J_i^{max} : i \in \{1, \ldots, N\}, i \neq j\} < J_j^{min}, \quad (33)$$

where

$$J_i^{max} \triangleq \max\left\{(\hat{z}_i)' P \hat{z}_i : \hat{z}_i \in \hat{S}_i\right\} \quad (34)$$

$$J_j^{min} \triangleq \min\left\{(\hat{z}_j)' P \hat{z}_j : \hat{z}_j \in \hat{S}_j^F\right\}. \quad (35)$$

Then, under the fault scenario of Assumption 4.3, the closed-loop dynamics of the multisensor switching scheme described in Section II remain stable in the event any sensor fails.

Proof: Suppose that a jth sensor fails. At the sampling instant following the fault, Condition 1) of Assumption 4.3 guarantees that there exists at least one operational lth sensor that has the states of the corresponding estimator tracking error subsystem (22) in the invariant set $\hat{S}_l$. In addition, Assumption 4.4 guarantees that Condition 2) of Assumption 4.3 is fulfilled at the sampling instant following the time of the fault, i.e., the states of the estimator tracking error subsystem corresponding to the failed sensor are in $\hat{S}_j^F$. Conditions (33)–(35) then ensure that the lth sensor has smaller cost than the failed jth sensor and thus the latter cannot be selected by the switching mechanism (19). It follows that at the sampling instant following the time of the fault the controller selects any of the available healthy sensors (not necessarily the lth sensor) which, by Condition 1) of Assumption 4.3 have estimation errors inside $\tilde{S}_i$ (25), hence satisfying the bounds (26). Thus Assumption 4.2 holds at the sampling instant following the time of the fault and the analysis of Section IV-A shows that the states of the estimator tracking error subsystems corresponding to healthy sensors and to the failed jth sensor remain in $\hat{S}_i$ and $\hat{S}_j^F$, respectively. The previous argument can be repeated inductively for the duration of the fault, concluding that the switching controller never selects faulty sensors to implement the control law and that the resulting dynamics remain in the respective invariant sets. The result then follows. ■

Remark 4.6: Note that Fault Detection and Identification (FDI), a feature normally needed in fault tolerant control, is performed *implicitly* via the switching mechanism (19), through satisfaction of the pre-checkable conditions of Assumption 4.4 and (33)–(35). (In effect, as was proven in the previous theorem, under those conditions the switching mechanism exclusively selects healthy sensors.)

V. NUMERICAL EXAMPLE

We consider here the longitudinal control problem for a *stop-and-go scenario*. In this scenario, the follower car follows the leader car at a safe reference inter-distance [5]; the sudden accelerations and decelerations produce important variations of the inter-distance and its time-derivatives. The interdistance dynamics are represented by the discretisation of a double integrator plant, for a sample period of $0.1s$, and satisfy (3) with $A = \begin{bmatrix} 1 & 0.1 \\ 0 & 1 \end{bmatrix}$, $B = [0\ 0.1]'$, $E = B$ and $|w| \leq 0.01$. For simplicity, the two sensors have the same characteristics, i.e. $C_i = C = [1\ 0]$. The sensor noises are bounded as follows: $|\eta_i| \leq 0.02$, $|\eta_i^F| \leq 0.02$ [cf. (28)], for $i = 1, 2$. The estimators are given by (11) with $L_i = [1.5\ 5.4]'$, (computed by pole placement). The Jordan decompositions $A_{L_i} = V_i \Lambda_i V_i^{-1}$ are computed using Matlab's *eig* function. The controller is designed as in Section II-E, with $K = [20\ 9.0]$. Using the interdistance reference model of [5] the problem data gives an elementwise bounded reference tracking signal $[3\ \ -3]' \leq x_{ref} \leq [18\ 3]'$.

With the above data, Assumption 4.4 and Conditions (33)–(35) are satisfied. Hence the system is guaranteed to be closed-loop stable under sensor fault. A geometric inter-

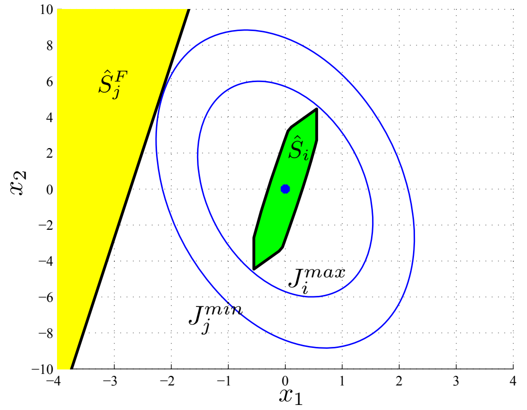

Fig. 3. Geometric interpretation of the multisensor switching stability Conditions (33)–(35) for longitudinal control.

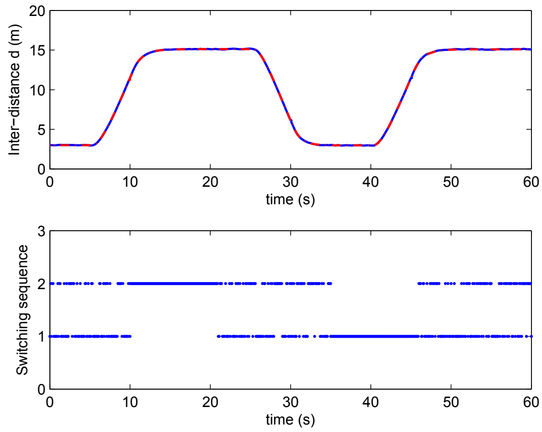

Fig. 4. a) Inter-distance reference signal (dotted) and actual inter-distance (solid) b) Switching sequence.

pretation of Conditions (33)–(35), is illustrated in Figure 3. The distance between J_j^{min} and J_i^{max} may be interpreted as a *robust margin* for fault-tolerance.

In the simulation, each sensor fails for a period of $10s$ and then recovers, with no fault periods overlapping between sensors (since we require at least one operational sensor at all times). Sensor 1 fails during $10 \leq t \leq 20$ and sensor 2 fails during $35 \leq t \leq 45$. Figure 4a) depicts the interdistance reference signal (dotted) and the actual interdistance between vehicles (solid). The switching sequence, shown in Figure 4b), commutes between both sensors in the absence of fault and chooses exclusively the healthy sensor during faults. Figure 5 depicts the individual costs corresponding to each sensor, used in equation (19) to implement the switching law. Notice that the switching system exhibits a stable behaviour.

VI. Conclusions

We have presented a multi-sensor switching strategy for automotive longitudinal control. The proposed switching strategy is able to maintain the performance and the stability of the system, even under the occurrence of severe faults

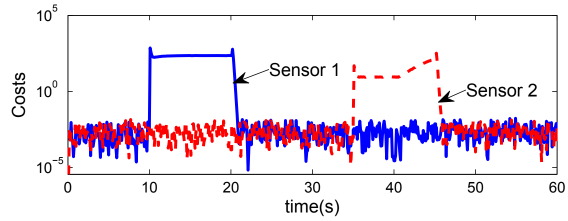

Fig. 5. Individual costs corresponding to each sensor.

in some of the sensors, by selecting, at each time instant, a sensor (belonging to a family of sensors) that provides the best closed loop performance according to an optimisation criterion. An important property of this approach is that the individual controllers (estimators plus state feedback gain) are designed for the fault-free case without taking into account the possibility of fault occurrence.

The construction of ultimate-bound invariant sets is a key issue for establishing fault-tolerant properties. Recent refinements for constructing such sets (e.g. [12], [13]), introduce less conservatism in the set-invariance analysis. This paper has illustrated the applicability of the proposed scheme.

References

[1] Martínez J.J., Zhuo X.W., De Doná J.A., and Seron M.M. “Multisensor switching strategy for automotive longitudinal control”. In *Proc. of the 2006 American Control Conference*, Minneapolis, MN, USA, 2006.

[2] Seron M.M., Zhuo X.W., De Doná J.A., and Martínez J.J. “Fault tolerant multisensor switching control strategy”. *European Control Conference*, 2007.

[3] Stoustrup J. and Niemann H. “Fault tolerant feedback control using the youla parametrization”. *In: Proceedings of the 6th European Control Conference (ECC01). Porto, Portugal*, 2001.

[4] Vahidi A. and Eskandarian A. “Research Advances in Intelligent Collision Avoidance and Adaptive Cruise Control”. *IEEE Trans. Intell. Transp. Syst.*, Vol.4, No.3, pp. 143-153, Sept. 2003.

[5] Martinez J.J. and Canudas de Wit C., “A Safe Longitudinal Control for Adaptive Cruise Control and Stop-and-Go Scenarios”. *IEEE Transactions on Control Systems Technology*, Vol.15, No.2, March 2007.

[6] Kam M., Zhu X. and Kalata P., “Sensor fusion for mobile robot navigation”. *Proc. IEEE*, pp. 108-118, Vol.85, No.1, Jan. 1997.

[7] Ren C. Luo, Chih-Chen Yih, and Kuo Lan Su. “Multisensor fusion and integration: approaches, applications, and future research directions”. *IEEE Sensors Journal*, 2(2):107-119, April 2002.

[8] Shu-li Sun. Multi-sensor optimal information fusion kalman filters with applications. *Aerospace Science and Technology*, 8(1):57-62, January 2004.

[9] Zhou K. and Ren Z., “A New Controller Architecture for High performance, Robust, and Fault-Tolerant Control”. *IEEE Trans. Autom. Control*, pp.1613-1618, Vol.46, No.10, October 2001.

[10] Isermann R. “Process Fault Detection Based on Modeling and Estimation Methods - A Survey”. *Automatica*. Vol.20. No.4. pp.387-404. 1984.

[11] Yame J. and Kinnaert M. “Supervisory Fault-Tolerant Control With Application to the IFATIS Two-Tanks Benchmark”. *IFAC World Congress*, Prague 2005.

[12] Kofman E.J., Haimovich H. and Seron M.M. “A Systematic Method to Obtain Ultimate Bounds for Perturbed Systems”. *International Journal of Control*, Vol.80, No.2, pp.167-178, February 2007.

[13] Olaru S., De Doná, J.A. and Seron, M.M.“Positive invariant sets for fault tolerant multisensor control schemes”. In *Proceedings 17 IFAC World Congres*, Seoul, Korea, July 2008.

[14] Seron, M.M., Zhuo, X.W., De Doná, J.A. and Martínez, J.J. “Multisensor switching control strategy with fault tolerance guarantees” *Automatica*, Vol.44, No.1, pp. 88–97, 2008.